engaged in extensive contacts to amino acids within domain Ia, specifically to the constellation of five residues that were found to be essential for the adenylyltransferase activity of *E. coli* LigA. The nicotinamide base is sandwiched in a π stack between two conserved tyrosines. An invariant asparate makes a hydrogen bond to the amide nitrogen of nicotinamide. Another invariant aspartate coordinates the ribose 2′ O, and a tyrosine (or a histidine in *Eco*LigA) donates a hydrogen bond to the NMN phosphate. At first sight, the NMN binding site appears eminently "drugable."

The surprising finding made by Gajiwala and Pinko was that exposure of their crystal of NMN bound LigA to 100 mM AMP resulted in a rearrangement of the crystal lattice, caused by a large rigid-body rearrangement of domain Ia into a closed conformation, entailing an impressive 80 Å movement of the N terminus of the protein and resulting in de novo synthesis of NAD^+ in the active site by reaction of the bound NMN with AMP (Figure 1B). This reaction had not been described previously for any polynucleotide ligase, the novelty being that reversal of the ligase adenylylation reaction normally entails attack of NMN (or pyrophosphate in the case of ATP-dependent ligases) on the covalent lysyl-AMP intermediate. Here, instead, the unadducted AMP is chemically reactive with NMN. An interesting question is whether the phosphoanhydride bond in NAD^+ is generated by a single-step mechanism (direct attack) or through a lysyl-AMP intermediate. It is also fascinating that NAD^+ synthesis occurs in the absence of an exogenous divalent cation, which is essential for the normal ligase adenylylation reaction. The finding that a domain fragment of LigA can effect a chemical transformation of AMP is reminiscent of the presence of AMP in the active site of bacteriophage T4 RNA ligase 2 that was crystallized in the absence of added nucleotide (Ho et al., 2004). In that case, the AMP was apparently generated by hydrolysis of the ligase-adenylate adduct within the crystal. An emerging theme is either that the isolated domains of polynucleotide ligases are capable of novel reactions not described for the full-length proteins or that in silico conditions are themselves conducive to revealing novel reactions.

The structure of the LigA-NAD^+ complex reveals that domain closure creates a new interface between the Ia and nucleotidyl transferase modules, thereby providing another potential target for interference with LigA activity by a small molecule. Brötz-Oesterhelt et al. (2003) have conducted a high throughput screen that identified pyridochromanones as inhibitors of LigA function in vitro and in vivo. Although inhibition was reportedly competitive with respect to NAD^+, a LigA mutation conferring resistance to pyridochromanone was mapped to a single amino acid change in a domain distal to the Ia and nucleotidyltransferase modules. Obviously, the structure of a LigA-pyridochromanone complex would be highly informative. We can anticipate that the present structural characterization of the NMN binding site in domain Ia will fuel efforts to discover new small molecules that compete for this site.

Stewart Shuman
Molecular Biology Program
Sloan-Kettering Institute for Cancer Research
New York, New York 10021

Selected Reading

Brötz-Oesterhelt, H., Knezevic, I., Bartel, S., Lampe, T., Warnecke-Eberz, U., Ziegelbauer, K., Häbich, D., and Labischiinski, H. (2003). J. Biol. Chem. *278*, 39435–39442.

Gajiwala, K., and Pinko, C. (2004). Structure *12*, this issue, 1449–1459.

Ho, C.K., Wang, L.K., Lima, C.D., and Shuman, S. (2004). Structure *12*, 327–339.

Lee, J.Y., Chang, C., Song, H.K., Moon, J., Yang, J., Kim, H.K., Kwon, S.T., and Suh, S.W. (2000). EMBO J. *19*, 1119–1129.

Odell, M., Sriskanda, V., Shuman, S., and Nikolov, D.B. (2000). Mol. Cell *6*, 1183–1193.

Sriskanda, V., and Shuman, S. (2002). J. Biol. Chem. *277*, 9685–9700.

Wilkinson, A., Day, J., and Bowater, R. (2001). Mol. Microbiol. *40*, 1241–1248.

Structure, Vol. 12, August, 2004, DOI 10.1016/j.str.2004.07.003

Complete Three-Dimensional Structures of Picornaviral RNA-Dependent RNA Polymerases

In this issue of *Structure*, Love et al. report the three-dimensional structures of the RNA-dependent RNA polymerase (RdRp), 3Dpol, from three different human rhinovirus serotypes.

Although they differ by as much as 50% in sequence, the polymerases encoded by human rhinovirus (HRV) 14, HRV16, and HRV1b, solved at 2.8, 2.5, and 2.3 Å resolution, respectively, are nearly superimposable with each other and with a new structure of the polymerase of poliovirus, recently solved to 2.0 Å resolution by Thompson and Peersen (2004). These new structures differ from the previously published three-dimensional structure of the poliovirus RdRp (Hansen et al., 1997) in that virtually all amino acids are resolved, because both new groups achieved crystallization conditions that immobilized the extremely flexible N-terminal sequences of the molecules, yielding crystals. In the case of the

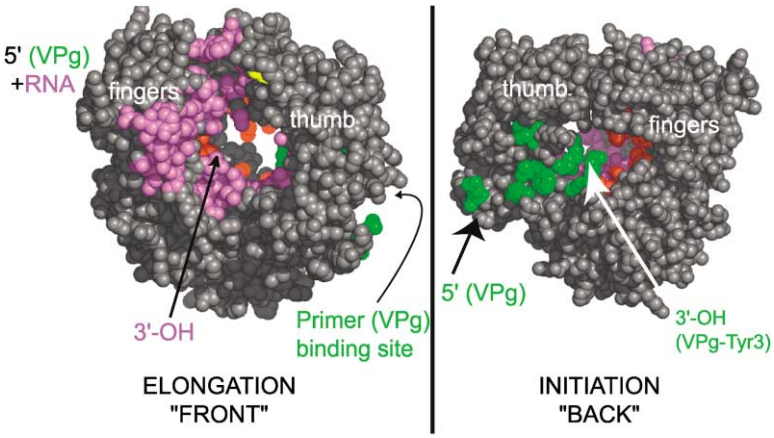

Figure 1. Known and Predicted Substrate Binding Sites on the Newly Determined Three-Dimensional Structures of Three Rhinoviruses (Love et al., 2004) and Poliovirus (Thompson and Peersen, 2004)

Green: Residues implicated in primer (VPg) uridylylation, in the binding of the VPg precursor, 3AB, or both (Lyle et al., 2002b). Yellow: Asp-406, implicated in binding the template for VPg uridylylation, the *cis*-acting replication element (CRE) (Yang et al., 2004). Red: Nucleotide binding pocket (Gohara et al., 2000). Pink: Template and nascent strand RNA binding residues, based upon homology modeling of the HRV-14 3D polymerase with the ternary complex of HIV reverse transcriptase, nucleotide, and primer:template strands (Huang et al., 1998). The same active site (red) is implicated in both uridylylation, the addition of UMP to the protein primer, VPg, and in the elongation of the VPg-bound primer strand, although these substrates are predicted to bind to opposite faces of the molecule. Poliovirus polymerase coordinates kindly provided by O. Peersen.

poliovirus polymerase, this was achieved by the mutation of two amino acids at an intermolecular interface termed "Interface I" by Hansen et al. (1997).

An Encircled Active Site for All RNA-Dependent RNA Polymerases

Polymerase structures have been likened to right hands, with the active site in the conserved "palm" domain and the template strand traversing the front of the palm (Huang et al., 1998). As the structures of more polymerases in active conformations become available, the positioning of these "hands" becomes increasingly clenched. As foreshadowed by the structures of RNA-dependent RNA polymerases from other positive-strand RNA viruses such as hepatitis C virus (HCV), bovine viral diarrhea virus and the most closely related to picornaviral polymerases, rabbit hemorrhagic fever virus, the amino-terminal sequences of all four picornaviral RdRps in the new crystal structures traverse from the top of the fingers to the top of the thumb, then back again to the fingers domain. With an encircled active site, it is likely that template and primer molecules contacting the "front" face of the polymerase use the opening in the middle of the polymerase primarily for nucleotide exchange, as has been shown for reverse transcriptase and other polymerases (see Figure 1).

Proteolytic Activation of Polymerase Activity

Picornaviral proteins are translated from a single open reading frame to yield a polyprotein that is subsequently cleaved into limited digestion products by viral proteases. Stable intermediate digestion products include 3CD, which may be further cleaved to produce 3C protease and 3D polymerase. Although 3CD is active as a protease, it is completely inactive as a polymerase. How is 3D polymerase activity suppressed in 3CD and larger precursors and subsequently activated upon proteolysis? The answer becomes apparent upon inspection of the new 3D polymerase structures. The N-terminal glycine residue in the 3Dpol structures are buried and participate extensively in hydrogen-bond networks within the fingers domains that include highly conserved residues such as Gly-64, Gly-284, and Gly-285. In the HRV1b polymerase structure, the N-terminal glycine is also close to a putative potassium binding site, which Love et al. suggest might stabilize the N-terminal association. Thompson and Peersen (2004) also solved the structure of poliovirus 3Dpol molecules in which the N-terminal 68 amino acids were deleted and in which the N-terminal Gly was changed to Ala. Based upon these structures, they argue that the N-terminal Gly pushes a conserved nucleotide binding residue, Asp-238, a distance of 1.4 Å into the catalytic site, perhaps thereby physically coupling the formation of a complete active site to proteolytic processing of 3CD. Interestingly, one of the residues in the hydrogen-bonding network that extends from Gly-1 to Asp-238 is Gly-64. That a G64S mutation was shown to increase the fidelity of poliovirus RNA replication (Pfeiffer and Kirkegaard, 2003) lends further support to the functionality of nucleotide orientation by the hydrogen-bonding network that extends from the proteolytically generated N-terminal Gly to the active site.

Oligomerization at Interface I

Hansen et al. (1997) described a significant degree of surface burial (1480 Å^2) between the thumb of one polymerase and the back of the palm of another, which they termed "Interface I." Iteration of this interface in a head-to-tail fashion leads to the formation of polymerase fibers of indeterminate length, 50 Å in width. Cooperative effects of polymerase concentration on RNA binding and enzymatic activity also provided biochemical evidence consistent with oligomerization of the poliovirus polymerase, and mutations in either the "thumb" or "palm" side of the poliovirus polymerase produced either non-viable or small-plaque virus (Hobson et al., 2001; Pathak et al., 2002). Fibers and sheets of poliovirus 3Dpol have been observed by electron microscopy and solutions of 3Dpol create turbidity in light absorption experiments akin to that produced by microtubules (Lyle et al., 2002a). Certain other viral RdRps, such as HCV NS5B, display oligomeric behavior as well. Is oligomerization via Interface I a conserved feature of picornaviral polymerases? Love et al. noted that a significant surface area (1010 Å^2) is buried in the crystal contacts of HRV14 3D polymerase and that many hydrophobic residues in this intermolecular interface are identical or similar to those observed in Interface I of poliovirus polymerase.

Interestingly, although no such large surface area is buried in the structures of HRV16 and HRV1b polymerases, many of the residues involved in potential Interface I surfaces (Ile- or Leu-446, Arg- or His-454, and Arg- or Glu-455 on the thumb side and Asp-338 and Asp-, Asn-, or Lys-349 on the palm side) are similar or conserved among all picornaviral polymerases.

A Second Oligomeric Interface?

The extreme extension of the fingers domain N-terminal sequences (44 Å) required for enclosure of the active site had led Hansen et al. (1997), in whose structure the N-terminal residues contacting the thumb were resolved but the connection to the fingers was not, to hypothesize that the N-terminal residues over the thumb were donated intermolecularly. Experimental support for this hypothesis was provided by the observation of intermolecular crosslinking between poliovirus polymerase cysteines engineered at Ala-29 and Ile-441 (Hobson, et al. 2001). Furthermore, electron microscopic observation of oligomeric sheets of purified polymerase implied that a second set of contacts must exist to align fibers of polymerase formed along Interface I. Since all RNA viruses replicate on intracellular membranes, the existence of a flat, catalytic lattice is an attractive concept for membrane-associated RNA replication and, in support of this hypothesis, polymerase-containing oligomeric structures reminiscent of those seen with purified 3Dpol were observed on the surface of vesicles isolated from poliovirus-infected cells (Lyle et al., 2002a). What is the molecular nature of the contacts that hold these oligomeric structures together? The three rhinovirus polymerase structures and the full-length poliovirus polymerase structure clearly demonstrate intramolecular folding of the N-terminal residues and provide no hint for a potentially alternative second interface. Of course, this does not mean that interpolymerase contacts that create or stabilize a two-dimensional array in solution or on a membrane surface do not exist, and may be difficult to stabilize in a three-dimensional crystal. In this context, it is interesting that resolution of the fingers domain of the poliovirus polymerase required disruption of Interface I (Thompson and Peersen, 2004). Further experimentation is required to determine the nature of the molecular contacts between polymerase monomers, precursors, and polymers in the context of the membrane-associated RNA replication complex. The new molecular surfaces revealed by these full-length structures will be invaluable in these investigations.

Phosphodiester Bond Formation with Substrates on Opposite Sides of the Active Site

Using the new full-length structures, existing genetic data from several picornaviruses, and homology with other polymerases, Love et al. modeled the binding of NTP and a primer-template duplex into the HRV14 polymerase active site, and Thompson and Peersen modeled the binding of a template strand to poliovirus 3Dpol. In Figure 1, we have highlighted the residues of poliovirus polymerase, all on the "front" face of the polymerase, expected to contact the template and primer. Love et al. noted that modeling a template-primer duplex required little adjustment of the HRV14 polymerase structure, and speculated that only slight conformational change might be involved during substrate binding and phosphodiester bond formation for this class of polymerases. Indeed, some RNA-dependent RNA polymerases, such as those from bacteriophage ϕ6, reovirus, HCV, and bovine viral diarrhea virus, do not require a primer and are thought to possess a natural affinity for the nucleotides present at the 5′ ends of their viral genomes. These de novo-initiated strands must then rearrange to bring the nascent 3′-OH ends in close proximity to the nucleotide tunnel and the template strand, where further additions may occur during elongation; for the reovirus and ϕ6 polymerases, this process requires only modest conformational change (Butcher et al., 2001; Tao et al., 2002).

The conformational change from initiation to elongation in picornaviral polymerases, however, is likely to be especially dramatic, and its mechanism remains unknown. Picornaviruses such as rhinovirus and poliovirus use a 22-amino acid protein primer, VPg (3B), to initiate RNA replication (Paul et al., 1997). RNA synthesis, primed by uridylylation of Tyr-3 of VPg, is predicted to use the same catalytic aspartates at the polymerase active site as those used for internucleotide bond formation. The binding site on poliovirus 3Dpol for the proteolytic precursor of VPg, 3AB, has been mapped to the back side of the palm near the base of the thumb (Lyle et al., 2002b; Figure 1). Love et al. noted the structural and sequence conservation of these residues in the rhinovirus polymerase (tequila aficionados will recognize this as the area where salt is placed on the drinker's right hand). Therefore, it is likely that nucleotide addition to VPg occurs through the opposite side of the nucleotide channel from RNA elongation. How is the uridylylated VPg primer transferred from the back to the front side of the polymerase? Intramolecularly, through the nucleotide channel? Intermolecularly, to another polymerase? How the two different substrates approach the active site from opposite sides, and how uridylylated VPg is rebound in elongation mode, are fascinating questions posed by these new structures.

Scott Crowder and Karla Kirkegaard
Department of Microbiology and Immunology
Stanford University School of Medicine
Stanford, California 94305

Selected Reading

Butcher, S.J., Grimes, J.M., Makeyev, E.V., Bamford, D.H., and Stuart, D.I. (2001). Nature *410*, 235–240.

Gohara, D.W., Crotty, S., Arnold, J.J., Yoder, J.D., Andino, R., and Cameron, C.E. (2000). J. Biol. Chem. *275*, 25523–25532.

Hansen, J.L., Long, A.M., and Schultz, S.C. (1997). Structure *5*, 1109–1122.

Hobson, S.D., Rosenblum, E.S., Richards, O.C., Richmond, K., Kirkegaard, K., and Schultz, S.C. (2001). EMBO J. *20*, 1153–1163.

Huang, H., Chopra, R., Verdine, G.L., and Harrison, S.C. (1998). Science *282*, 1669–1675.

Love, R.A., Maegley, D.A., Yu, X., Ferre, R.A., Lingardo, L.K., Diehl, W., Parge, H.E., Dragovich, P.S., and Fuhrman, S.A. (2004). Structure *12*, this issue, 1533–1544.

Lyle, J.M., Bullitt, E., Bienz, K., and Kirkegaard, K. (2002a). Science *296*, 2218–2222.

Lyle, J.M., Clewell, A., Richmond, K., Richards, O.C., Hope, D.A., Schultz, S.C., and Kirkegaard, K. (2002b). J. Biol. Chem. *277*, 16324–16331.

Pathak, H.B., Ghosh, S.K., Roberts, A.W., Sharma, S.D., Yoder, J.D., Arnold, J.J., Gohara, D.W., Barton, D.J., Paul, A.V., and Cameron, C.E. (2002). J. Biol. Chem. *277*, 31551–31562.

Pfeiffer, J.K., and Kirkegaard, K. (2003). Proc. Natl. Acad. Sci. USA *100*, 7289–7294.

Paul, A.V., van Boom, J.H., Fillippov, D., and Wimmer, E. (1998). Nature *393*, 280–284.

Tao, Y., Farsetta, D.L., Nibert, M.L., and Harrison, S.C. (2002). Cell *111*, 733–745.

Thompson, A.A., and Peersen, O.B. (2004). EMBO J., in press.

Yang, Y., Rijnbrand, R., Watowich, S., and Lemon, S.M. (2004). J. Biol. Chem. *279*, 12659–12667.

Structure, Vol. 12, August, 2004, DOI 10.1016/j.str.2004.07.004

The Evolving Role of 3D Domain Swapping in Proteins

3D domain swapping is increasingly implicated in amyloidosis but also has potential functional advantages in soluble proteins. Indeed, the structure of an NF-κB p50 mutant (Chirgadze et al., 2004) demonstrates that 3D domain swapping can rescue function after a destabilizing mutation. This work has wider implications for the evolution of protein oligomers.

3D domain swapping is a mechanism for forming dimers or higher oligomers by exchanging protein domains that remain covalently connected to the core domain through the polypeptide chain (Bennett et al., 1995). A 3D domain-swapped dimer (Figure 1A, top right) resembles the native closed monomer (Figure 1A, left) in its overall domain arrangement; however, the interdomain interface in the dimer is formed by two independent protein chains. The only segment of the domain-swapped dimer that differs in conformation from the closed monomer is the hinge loop. Higher order multimers can also form by 3D domain swapping and may be closed-ended oligomers or open-ended fibrils (Figure 1A, bottom right). Structures of a number of 3D domain-swapped proteins have revealed that swapped domains can range from a short peptide to an entire globular domain. 3D domain-swapped proteins are characterized by unique structural and energetic properties as compared to conventional "side-by-side" dimers. For example, 3D domain swapping involves passing through an "open monomer" (Figure 1A, middle) or partially unfolded intermediate state. Because of this, domain-swapped proteins typically do not equilibrate with their closed monomer counterparts at an appreciable rate under standard conditions.

Since the introduction of the term "3D domain swapping" and its proposal as a general mechanism for interconverting protein monomers and higher oligomers (e.g., Bennett et al., 1995), more than forty domain-swapped or potentially domain-swapped proteins have been structurally characterized (reviewed in Liu and Eisenberg, 2002). The variety of such proteins suggests that 3D domain swapping facilitates diverse functions in vivo. There is increasing evidence that 3D domain swapping is involved in the formation of fibrils from amyloidogenic proteins (e.g., Lee and Eisenberg, 2003; Nilsson et al., 2004). 3D domain swapping may also be involved in benign processes, including some types of allosteric regulation, conformational switching, complementation at active sites and evolution of oligomers, although evidence for such roles has been mostly indirect.

The paper by Chirgadze et al. (2004) in this issue demonstrates that 3D domain swapping is a mechanism for evolving functional protein oligomers. Specifically, their work reveals that 3D domain swapping rescues function in a mutant of dimeric NF-κB p50, a member of the Rel family of transcription factors. Previously, Hart et al. (2001) identified 25 mutants of NF-κB p50 by screening a library of proteins with random mutations at the dimer interface (residues Y267, L269, A308, and V310). The mutant proteins with "novel functional interfaces" dimerized successfully and retained DNA binding properties similar to wild-type NF-κB p50.

Chirgadze et al. (2004) have determined the crystallographic structures of six of these mutants using a dimerization domain-only construct (residues 245–350). Five of the six mutants closely resemble the wild-type NF-κB p50 structure, which is a side-by-side dimer (Figure 1B, left and bottom right); however, one mutant (MLAM) is 3D domain swapped (Figure 1B, top right). The domain-swapped MLAM dimer is highly intertwined; the exchanged domain comprises three β strands that form half of an Ig-like fold. Thus, the structure is reminiscent of domain-swapped CD2, which exchanges four strands in an Ig-like fold (Murray et al., 1995). The highly intertwined structure of MLAM suggests that it is an obligate homodimer that forms during folding, similar to several other domain-swapped proteins (reviewed in Rousseau et al., 2003). In contrast, the wild-type NF-κB p50 homodimer has a micromolar K_d, characteristic of weak dimerization (Sengchanthalangsy et al., 1999), which may contribute to its ability to heterodimerize with other Rel family members. The obligate MLAM homodimer would not be expected to form heterodimers in cells, which could lead to different downstream effects.

The work of Chirgadze et al. (2004) confirms previous observations that one or a few amino acid replacements can lead to 3D domain swapping (reviewed in Rousseau et al., 2003) and provides a speculative estimate of the frequency with which 3D domain swapping occurs in nature. Comparison of wild-type NF-κB p50 with domain-swapped MLAM reveals that two amino acid replacements, at positions 267 and 310, lead to 3D domain